

# Influence of volume fraction on fracture mechanism of Al-Al<sub>4</sub>C<sub>3</sub> system studied by “in-situ tensile test in SEM”

M. Besterčí<sup>1</sup>, O. Velgosová<sup>2\*</sup>, J. Ivan<sup>3</sup>, P. Hvizdoš<sup>1</sup>, I. Kohútek<sup>4</sup>

<sup>1</sup>*Institute of Materials Research, Slovak Academy of Sciences, Watsonova 47, 043 53 Košice, Slovak Republic*

<sup>2</sup>*Dept. of Non-ferrous Metals and Waste Treatment, Faculty of Metallurgy, Technical University, Letná 9/A, 042 00 Košice, Slovak Republic*

<sup>3</sup>*Institute of Materials and Machine Mechanics, Slovak Academy of Sciences, Račianska 75, 831 02 Bratislava, Slovak Republic*

<sup>4</sup>*Research and Testing Institute, U. S. Steel Košice, 044 54 Košice, Slovak Republic*

Received 18 January 2008, received in revised form 15 March 2008, accepted 18 March 2008

## Abstract

The method of “in-situ tensile testing in SEM” is suitable for investigations of fracture mechanisms because it enables to observe and document deformation processes directly, and so the initiation and development of plastic deformation and fracture can be reliably described. With increasing tensile load, local cracks are formed by rupture of large particles and decohesion of smaller particles. Further increase of load leads to the crack growth by coalescence of cavities in the direction from the surface into the specimen centre. Depending on the particle volume fraction, the cracks can be parallel or perpendicular to the load direction. The final rupture takes place in rows of variable density, depending on the volume fractions of carbide (Al<sub>4</sub>C<sub>3</sub>) and oxide (Al<sub>2</sub>O<sub>3</sub>) particles.

The aim of the present study is to evaluate the influence of volume fraction of Al<sub>4</sub>C<sub>3</sub> particles (8 and 12 vol.%) on the fracture mechanism.

**Key words:** metal matrix composites, dispersion strengthened Al, “in-situ tensile testing in SEM”, fracture mechanisms

## 1. Introduction

The dispersion strengthened alloys Al-Al<sub>4</sub>C<sub>3</sub> manufactured by mechanical alloying using powder metallurgy technology are promising structural materials that enable significant weight cut for use first of all in aircraft and automobile industry and also at elevated temperatures.

In our previous works [1–7] and following [8–10] we used “in-situ tensile test in SEM” to analyse deformation processes in various types of Cu and Al based composites. In works [1, 7] the strain and fracture of Al-Al<sub>4</sub>C<sub>3</sub> system were studied. The influence of Al<sub>2</sub>O<sub>3</sub> vol.% in Cu-Al<sub>2</sub>O<sub>3</sub> system was analysed in [2, 5, 6]. Deformation process of Cu-TiC system was investigated in [3, 4]. In [8–10] Al-Si-Fe and Al-Si systems were studied by “in-situ tensile test in SEM”. The result was a design of several models of damage, which con-

sidered physical parameters of matrix and particles, as well as geometry and distribution of secondary phases.

## 2. Experimental materials and methods

The experimental materials were prepared by mechanical alloying. Al powder of powder particle size of < 50 μm was dry milled in an attritor for 90 min with the addition of graphite KS 2.5 thus creating 8 and 12 vol.% of Al<sub>4</sub>C<sub>3</sub>. The specimens were then cold pressed using a load of 600 MPa. The specimens had cylindrical shape. Subsequent heat treatment at 550 °C for 3 h induced chemical reaction 4Al + 3C → Al<sub>4</sub>C<sub>3</sub>. The cylinders were then hot extruded at 600 °C with 94 % reduction of the cross section. Due to a high affinity of Al to O<sub>2</sub> the system also contains a small amount of Al<sub>2</sub>O<sub>3</sub> particles. The volume

\*Corresponding author: tel.: 00421 55 602 24 27; fax: 00421 55 602 24 28; e-mail address: [oksana.velgosova@tuke.sk](mailto:oksana.velgosova@tuke.sk)

fraction of  $\text{Al}_2\text{O}_3$  phase was low, 1–2 vol.%. Detailed technology preparation is described in [11–14].

For the purposes of investigation very small flat tensile test pieces ( $7 \times 3$  mm) with 0.15 mm thickness were prepared by electroerosive machining, keeping the loading direction identical to the direction of extrusion. The specimens were ground and polished down to a thickness of approximately 0.1 mm. Finally, the specimens were finely polished on both sides by ion gunning. The test pieces were fitted into special deformation grips inside the scanning electron microscope JEM 100 C, which enables direct observation and measurement of the deformation by ASID-4D equipment. From each one of the systems (8 and 12 vol.% of  $\text{Al}_4\text{C}_3$ ) five samples were prepared.

### 3. Results and discussion

The microstructures of the materials with 8 and 12 vol.%  $\text{Al}_4\text{C}_3$  were fine-grained (the mean matrix grain size was  $0.35 \mu\text{m}$ ), heterogeneous, with  $\text{Al}_4\text{C}_3$  particles distributed in parallel rows as a consequence of extrusion. The average distance between the  $\text{Al}_4\text{C}_3$  particles found in thin foils was  $1.1 \mu\text{m}$ . Besides the phase  $\text{Al}_4\text{C}_3$ , the systems contained also  $\text{Al}_2\text{O}_3$  phase [11, 12, 14, 15]. Essentially, it was the remnant of oxide shells of the original matrix powder and/or shells formed during the reaction milling in attritors.

The phase analysis of the XRD spectra affirm apart from Al crystals the presence of aluminium carbide in Al-12vol.% $\text{Al}_4\text{C}_3$  material confirming the complete reaction of C after finishing of the composite preparation [16]. The systems contain also  $\text{Al}_2\text{O}_3$  phase detected by diffraction microanalysis.

When describing microstructures, one has to consider geometrical and morphological factors. According to the microstructure observations, the particles in our materials can be divided into three distinctive groups: A – small  $\text{Al}_4\text{C}_3$  particles, identified by TEM, Fig. 1, with mean size approximately 30 nm which made up to 70 % of the dispersoid volume fraction; B – large  $\text{Al}_4\text{C}_3$  particles with mean size between 0.4 and  $2 \mu\text{m}$ , found on metallographic micrographs; and C – large  $\text{Al}_2\text{O}_3$  particles with mean size of  $1 \mu\text{m}$ . Morphologically,  $\text{Al}_4\text{C}_3$  particles are elongated and  $\text{Al}_2\text{O}_3$  particles are spherical. Let us assume that particles of all categories during the high plastic deformation are distributed in rows. Mean distance between the rows is  $l$  and between the particles  $h$ . The particles are spherical or have only a low aspect ratio, so that they can be approximated as spherical. The experimental materials were deformed at  $20^\circ\text{C}$  at a rate of  $6.6 \times 10^{-4} \text{ s}^{-1}$  in the elastic region.

In the material with lower volume fraction (8 vol.%) of  $\text{Al}_4\text{C}_3$  with increase of the deformation load the initiation of microcracks on the large  $\text{Al}_4\text{C}_3$  particles

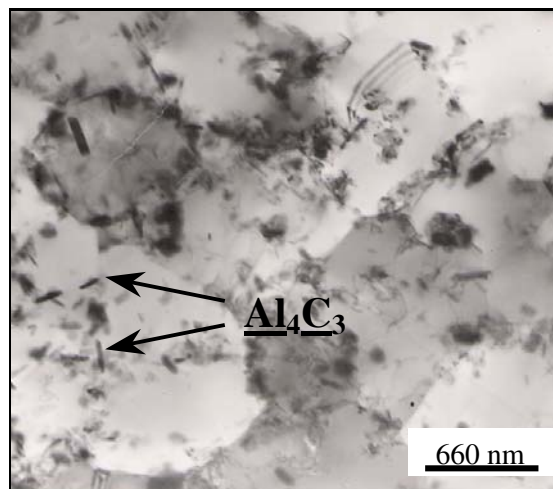


Fig. 1.  $\text{Al}_4\text{C}_3$  particles identified by TEM.

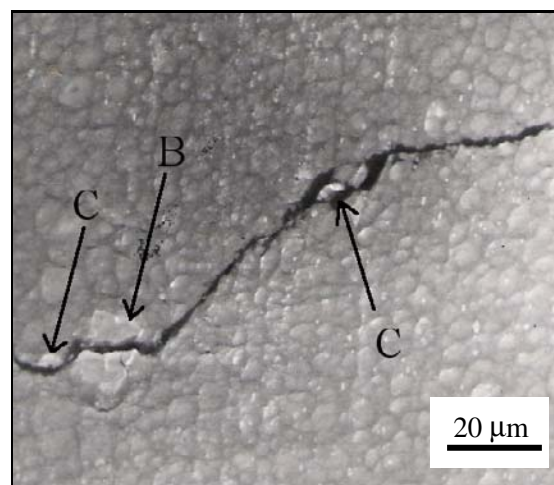


Fig. 2. Fracture path in the material with 8 vol.%  $\text{Al}_4\text{C}_3$ . Rupture of a large  $\text{Al}_4\text{C}_3$  grain and decohesion of the smaller particles (relative deformation  $\varepsilon = 0.12$ ).

(B) was observed to occur by their rupture simultaneously with decohesion of the smaller  $\text{Al}_4\text{C}_3$  and  $\text{Al}_2\text{O}_3$  particles C and B, Fig. 2. The fracture may be initiated on the surface of a specimen where large particles undergoing the damage are located. Cases of crack initiation by decohesion of large particles from the matrix and propagation of cracks towards the interior of the specimen were also observed, Fig. 3a,b. The crack then propagated from the surface into the bulk of the specimen.

In the case of the higher volume fraction (12 vol.%) of  $\text{Al}_4\text{C}_3$  the deformation process was very rapid due to the low plasticity of the material. The cracks were initiated on the surface and propagated approximately perpendicularly to the tensile load direction. Coalescence of the final fracture progressed along densely

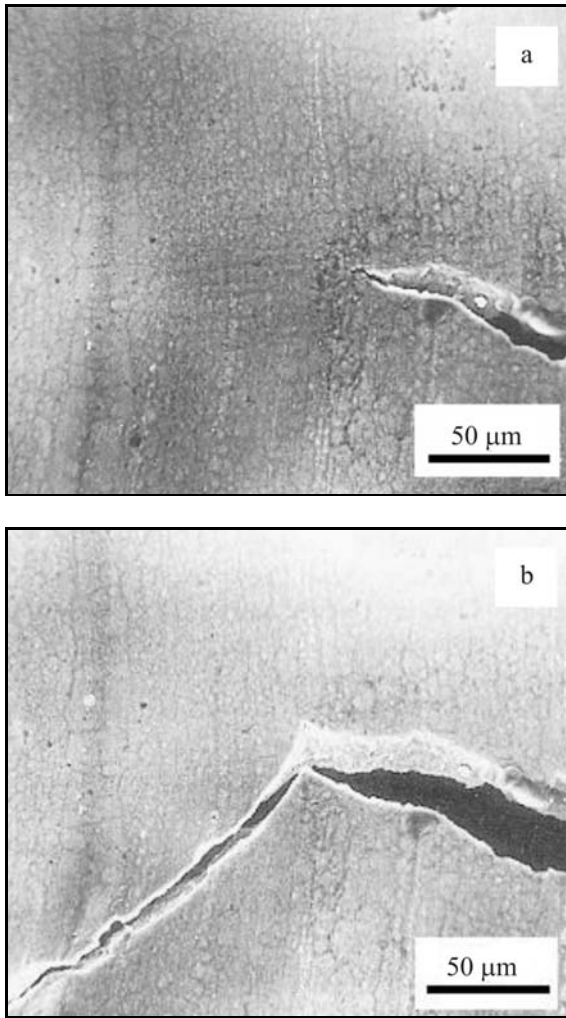


Fig. 3. Propagation of the fracture toward the specimen interior: a) relative deformation  $\varepsilon = 0.12$  mm; b) relative deformation  $\varepsilon = 0.185$  mm.

populated rows of  $\text{Al}_4\text{C}_3$  (A, B) particles parallel to the load direction, Fig. 4. The morphology and size of the deformed surface and three categories of particles on fracture surface can be seen in Fig. 5.

A detailed study of the deformation changes showed that the crack initiation was caused by decohesion, and occasionally also by rupture of the large particles. Decohesion is a result of different physical properties of different phases of the system. The Al matrix has significantly higher thermal expansion coefficient and lower elastic modulus (from  $23.5$  to  $26.5 \times 10^{-6} \text{ K}^{-1}$  and  $70 \text{ GPa}$ ) than both  $\text{Al}_4\text{C}_3$  ( $5 \times 10^{-6} \text{ K}^{-1}$  and  $445 \text{ GPa}$ ) and  $\text{Al}_2\text{O}_3$  ( $8.3 \times 10^{-6} \text{ K}^{-1}$  and  $393 \text{ GPa}$ ), respectively. Large differences in the thermal expansion coefficients result in high stress gradients, which arise on the interphase boundaries during the hot extrusion. Since  $\alpha_{\text{matrix}} > \alpha_{\text{particle}}$ , high compressive stresses can be expected. However, because the stress gradients arise due to the temperat-

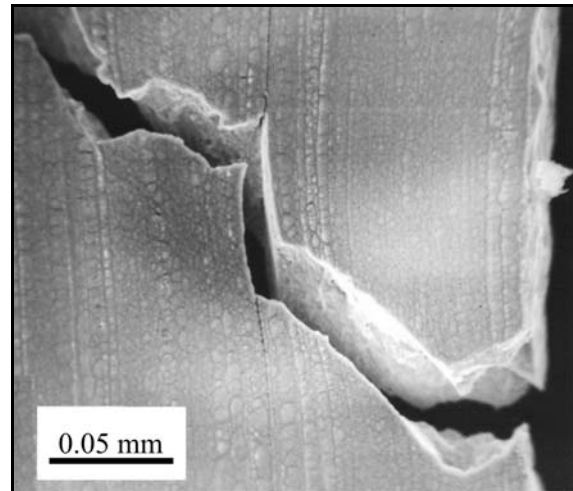


Fig. 4. Irregular fracture formed by a crack growing alternately along the particle rows and between them in the material with 12 vol.%  $\text{Al}_4\text{C}_3$  (relative deformation  $\varepsilon = 0.15$ ).

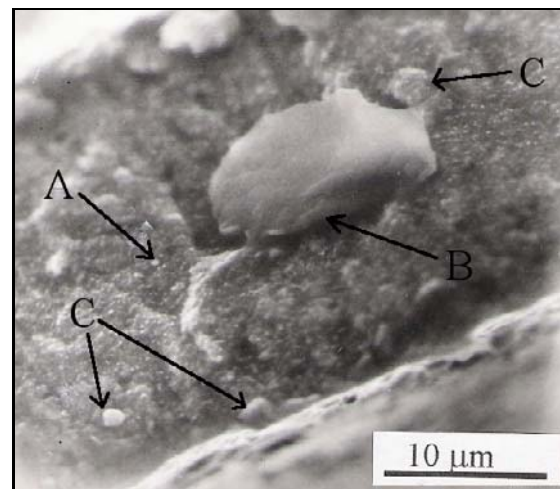


Fig. 5. Surface morphology of the material with 12 vol.%  $\text{Al}_4\text{C}_3$ .

ure changes, during cooling (which results in increase of the stress peaks) their partial relaxation can occur. Superposition of the external load and the internal stresses can initiate cracking at interphase boundaries.

In view of the dislocation theories the particles in composite may cause an increase in the dislocation density as a result of thermal strain mismatch between the ceramic particles and the matrix during preparation and/or thermal treatment. The difference between the coefficients of thermal expansion of the particles and the matrix may create the thermal residual stresses after cooling from the processing temperature to room temperature [17]. The coefficient of thermal expansion of the matrix is much higher

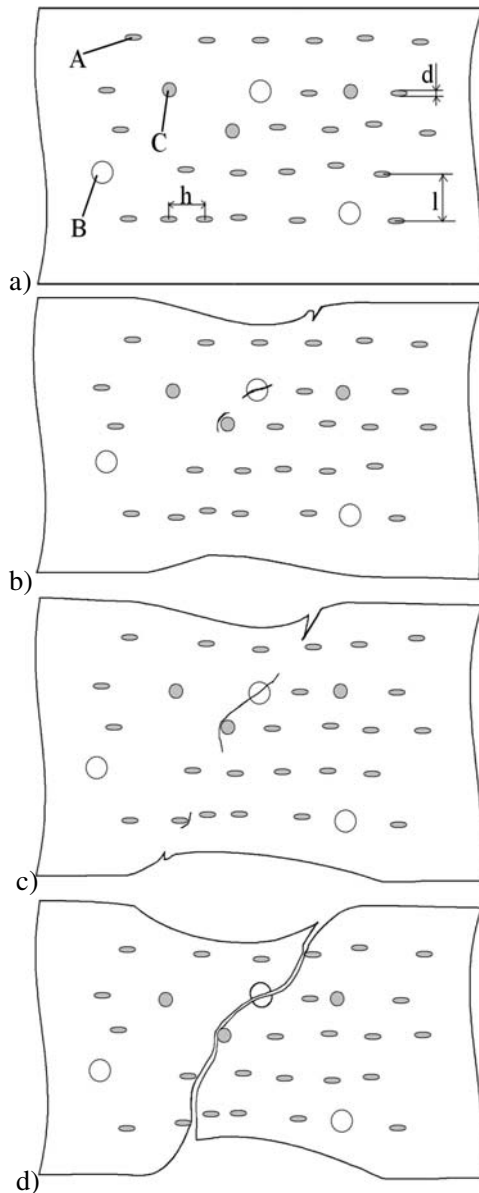


Fig. 6. Model of the fracture mechanism.

than that of the secondary particles. The thermal tension may relax around the matrix-particle interface by emitting dislocations. An increase in the dislocation density reinforcement has been calculated as

$$\Delta\rho = \frac{Bf\Delta\alpha\Delta T}{b(1-f)} \cdot \frac{1}{t}, \quad (1)$$

where  $\Delta\alpha$  is the difference of the coefficient of thermal expansion between matrix and particles,  $\Delta T$  is a temperature change,  $t$  is the minimum size of reinforcement,  $f$  is the volume fraction of particles,  $b$  is the magnitude of the Burgers vector of dislocations and  $B$  is a geometrical constant (depending on the aspect

ratio). The newly formed dislocations act as obstacles to the motion of dislocations in the matrix. Therefore a higher stress for the moving dislocations is necessary in comparison with materials without secondary particles.

From Eq. (1) it is obvious that the density of the newly created dislocations increases with an increase in the volume fraction. Therefore the number of obstacles for the dislocation motion increases and the stress necessary for the motion of dislocations increases, too. It should be mentioned that the effect of different types of secondary particles ( $\text{Al}_4\text{C}_3$ ,  $\text{Al}_2\text{O}_3$ ) on the reinforcement and damage depended not only on the coefficients of thermal expansion difference but also on the properties of the matrix/particle interface.

The fractures of the studied materials started at the side-edges of the deformed samples. When compared to the material with lower volume fraction of  $\text{Al}_4\text{C}_3$ , in the present system the development of slip bands in the bulk was inhibited. This fact, and the absence of long-range slips in the matrix, imply that the fracture is not inclined to the applied load but is perpendicular to it. This is caused by the high volume fraction of the strengthening particles and by their short distance. Considering the sample width (0.1 mm), the crack grew at  $45^\circ$  with respect to the sample surface. The fracture was transcrystalline, ductile.

Based on the microstructure changes observed in the process of deformation, the following model (it is not a general model but one that resulted from our experiments) of fracture mechanism is proposed on Fig. 6:

a) The microstructure in the initial state is characterized by  $\text{Al}_4\text{C}_3$  and  $\text{Al}_2\text{O}_3$  particles, categorized as A, B and C, whose geometric parameters ( $l$ ,  $h$  and  $d$ ) depend on their volume fraction.

b) With increasing tensile load, local cracks, predominantly on specimen side surfaces, are formed by rupture of large (B, C) and decohesion of smaller (A) particles.

c) Further increase of load leads to the crack growth by coalescence of cavities in the direction from the surface to the specimen centre. The cracks can be parallel or perpendicular to the loading direction, depending on the particle volume fraction.

d) The final rupture, i.e. interconnection of the side cracks along the loading direction, takes place in variably dense rows, depending on the volume fractions of carbide ( $\text{Al}_4\text{C}_3$ ) and oxide ( $\text{Al}_2\text{O}_3$ ) particles.

#### 4. Conclusion

The aim of the study was to evaluate the influence of volume fraction of  $\text{Al}_4\text{C}_3$  (8 and 12 vol.%) and  $\text{Al}_2\text{O}_3$  (1–2 vol.%) particles on the fracture mechan-

ism by means of the method “in situ tensile test in SEM”.

Based on the microstructure changes obtained in the process of deformation of the dispersion strengthened Al-Al<sub>4</sub>C<sub>3</sub> alloys, a model of fracture mechanism was proposed. With increasing tensile load the local cracks, predominantly on specimen's side surfaces, are formed by rupture of large (B, C) and decohesion of smaller (A) particles. Further increase of load leads to the crack growth by coalescence of cavities in the direction from the surface to the specimen centre. The orientation of cracks can be parallel or perpendicular to the loading direction, depending on the particle volume fraction. The final rupture, i.e. interconnection of the side cracks along the loading direction, takes place in variably dense rows, depending on the volume fractions of carbide (Al<sub>4</sub>C<sub>3</sub>) and oxide (Al<sub>2</sub>O<sub>3</sub>) particles.

The influence of volume fraction is evident on the change of geometric parameters of particle distribution in 3D, e.g. on the fracture kinetics. The mechanism of fracture does not depend in given range on the volume fraction of secondary particles.

#### Acknowledgements

The work was supported by the Slovak National Grant Agency under the Project VEGA 2/0105/08 and APVV-20-027205.

#### References

- [1] BESTERCI, M.—IVAN, J.: *J. of Mater. Sci. Lett.*, 15, 1996, p. 2071.
- [2] BESTERCI, M.—IVAN, J.: *J. of Mater. Sci. Lett.*, 17, 1998, p. 773.
- [3] BESTERCI, M.—IVAN, J.—KOVÁČ, L.—WEISS-GAERBER, T.—SAUER, C.: *Mat. Letters*, 38, 1999, p. 270.
- [4] BESTERCI, M.—IVAN, J.—KOVÁČ, L.—WEISS-GAERBER, T.—SAUER, C.: *Kovove Mater.*, 36, 1998, p. 239.
- [5] BESTERCI, M.—IVAN, J.—KOVÁČ, L.: *Kovove Mater.*, 38, 2000, p. 21.
- [6] BESTERCI, M.—IVAN, J.—KOVÁČ, L.: *Materials Letters*, 46, 2000, p. 181.
- [7] BESTERCI, M.—IVAN, J.—VELGOSOVÁ, O.—PEŠEK, L.: *Kovove Mater.*, 39, 2001, p. 361.
- [8] MOCELLIN, A.—FOUGEREST, F.—GOBIN, P. F. J.: *Mater. Sci.*, 28, 1993, p. 4855.
- [9] VELÍSEK, R.—IVAN, J.: *Kovove Mater.*, 32, 1994, p. 531.
- [10] BROUTMAN, L. V.—KROCK, R. H.: *Compos. Mater.*, 5, 1974, p. 27.
- [11] JANGG, G.—VASGURA, H.—SCHRÖDER, K.—ŠLESÁR, M.—BESTERCI, M.: In: *Int. Conf. PM, Düsseldorf 1986*, p. 989.
- [12] KORB, G.—JANGG, G.—KUTNER, F.: *Draht*, 30, 1979, p. 318.
- [13] ŠALUNOV, J.—ŠLESÁR, M.—BESTERCI, M.—OPPENHEIM, H.—JANGG, G.: *Metall*, 6, 1986, p. 601.
- [14] BESTERCI, M.: *Materials and Design*, 27, 2006, p. 416.
- [15] ĎURIŠIN, J.—ĎURIŠINOVÁ, K.—OROLÍNOVÁ, M.—BESTERCI, M.: *High Temp. Mat. and Processing*, 25, 2006, p. 149.
- [16] ĎURIŠIN, J.—OROLÍNOVÁ, M.—ĎURIŠINOVÁ, K.—BESTERCI, M.: *Kovove Mater.*, 45, 2007, p. 269.
- [17] LUKÁČ, P.—TROJANOVÁ, Z.: *Kovove Mater.*, 44, 2006, p. 243.